Real Time Observation of the Hydrothermal Crystallization of Barium Titanate Using in Situ Neutron Powder Diffraction

Richard I. Walton,[†] Franck Millange,[‡] Ronald I. Smith,[§] Thomas C. Hansen,[⊥] and Dermot O'Hare*[,#]

Contribution from the School of Chemistry, University of Exeter, Stocker Road, Exeter EX4 4QD, UK, Institut Lavoisier, UMR CNRS 8637, Université de Versailles Saint Quentin-en-Yvelines, 45 Avenue des Etats-Unis, 78035 Versailles Cedex, France, ISIS Facility, Rutherford Appleton Laboratory, Chilton, Oxon OX11 0QX, UK, Institut Laue Langevin, F-38042, Grenoble Cedex, France, and Inorganic Chemistry Laboratory, South Parks Road, Oxford OX1 3QR, UK

Received July 24, 2001

Abstract: The hydrothermal crystallization of barium titanate, $BaTiO_3$, has been studied in situ by time-resolved powder neutron diffraction methods using the recently developed Oxford/ISIS hydrothermal cell. This technique has allowed the formation of the ferroelectric ceramic to be followed in a noninvasive manner in real time and under genuine reaction conditions. In a first set of experiments, $Ba(OD)_2 \cdot 8D_2O$ was reacted with two different titanium sources, either crystalline TiO_2 (anatase) or amorphous $TiO_2 \cdot H_2O$ in D_2O, at 100−140 °C and the reaction studied using the POLARIS time-of-flight neutron powder diffractometer, at the ISIS Facility. In a second series of experiments, the reaction between barium chloride and crystalline TiO_2 (anatase) in $NaOD/D_2O$ was studied at temperatures between 100 and 200 °C and at different deuterioxide concentrations using the constant-wavelength D20 neutron powder diffractometer at the Institut Laue Langevin. Quantitative growth and decay curves were determined from analysis of the integrated intensities of Bragg reflections of starting materials and product phases. In both sets of experiments the rapid dissolution of the barium source was observed, followed by dissolution of the titanium source before the onset of crystallization of barium titanate. Using a nucleation-growth model we are able to simulate the growth curve of barium titanate at three temperatures. Our results indicate the predominance of a homogeneous dissolution−precipitation mechanism for the hydrothermal formation of barium titanate, rather than other possible mechanisms that have been discussed in the literature. Analysis of the line widths of the Bragg reflections in the neutron diffraction data indicates that the particle size of the $BaTiO_3$ product phase prepared from the amorphous $TiO_2 \cdot H_2O$ is smaller than that prepared from crystalline TiO_2 (anatase).

Introduction

The ferroelectric ceramic tetragonal barium titanate, *t*-$BaTiO_3$, finds widespread application as a capacitance material in the electroceramics industry. As well as its common use in multilayer capacitors, barium titanate also finds uses in components such as thermistors and electrooptic devices. Synthesis of the material is conventionally undertaken by solid-state reaction between titanium dioxide and barium carbonate at temperatures in excess of 900 °C. This simple procedure has a disadvantage in that it is difficult to control particle shape and size in the direct solid−solid reaction: often large particles with irregular morphologies are formed and this can have a detrimental effect on the electronic properties of the ceramics fabricated. Understandably, alternative routes to barium titanate formation have been investigated and the most widely studied of these is the hydrothermal reaction between barium-containing and titanium-containing solids, which takes place in basic solutions at temperatures as low as 80 °C (see for example work by Dutta and co-workers[1−3]). The hydrothermal method has allowed the production of fine powders (ranging in size from nanometers up to micrometers) with spherical morphology and narrow particle-size distributions[3−8] and the deposition of thin films of barium titanate.[9−11] The production of fine powders is of particular current interest because as well as enabling the formation of fine-grained ceramics by sintering the as-produced materials,[12] the fabrication of miniaturized devices has been postulated.[13,14]

[†] University of Exeter.
[‡] Université de Versailles Saint Quentin-en-Yvelines.
[§] Rutherford Appleton Laboratory.
[⊥] Institut Laue Langevin.
[#] Inorganic Chemistry Laboratory.

(1) Dutta, P. K.; Gregg, J. R. *Chem. Mater.* **1992**, *4*, 843.
(2) Dutta, P. K.; Asiasie, R.; Akbar, S. A.; Zhu, W. *Chem. Mater.* **1994**, *6*, 1542.
(3) Asiaie, R.; Zhu, W.; Akbar, S. A.; Dutta, P. K. *Chem. Mater.* **1996**, *8*, 226.
(4) Clark, I. J.; Takeuchi, T.; Ohtori, N.; Sinclair, D. C. *J. Mater. Chem.* **1999**, *8*, 83.
(5) Wu, M.; Long, J.; Wang, G.; Huang, A.; Luo, Y.; Feng, S.; Xu, R. *J. Am. Ceram. Soc.* **1999**, *82*, 3254.
(6) Um, M. H.; Kumazawa, H. *J. Mater. Sci.* **2000**, *35*, 1295.
(7) Lu, S. W.; Lee, B. I.; Wang, Z. L.; Samuels, W. D. *J. Cryst. Growth* **2000**, *219*, 269.
(8) Hu, M. Z.-C.; Kurian, V.; Payzant, E. A.; Rawn, C. J.; Hunt, R. D. *Powder Technol.* **2000**, *110*, 2.
(9) Slamovich, E. B.; Aksay, I. A. *J. Am. Ceram. Soc.* **1996**, *79*, 239.
(10) Kao, C. F.; Yang, C. L. *J. Eur. Ceram. Soc.* **1999**, *19*, 1365.
(11) Zeng, J.; Lin, C.; Song, Z.; Li, K.; Li, J. *Philos. Mag. Lett.* **2000**, *80*, 119.
(12) Pinceloup, P.; Courtois, C.; Leriche, A.; Thierry, B. *J. Am. Ceram. Soc.* **1999**, *82*, 3049.
(13) Hoffman, T.; Doll, T.; Fuenzalida, V. M. *J. Electrochem. Soc.* **1997**, *144*, L293.

10.1021/ja011805p CCC: $20.00
Published on Web 11/07/2001

If controlled growth of barium titanate powders with desired particle morphology is to be achieved, an understanding of the crystallization mechanism must be sought. Although several groups have investigated the hydrothermal crystallization of barium titanate in some detail,[15−19] no agreed description of its formation mechanism has been reached. Two extreme models have been put forward: one involving a homogeneous solution-phase reaction between titanium and barium hydroxy anions (the dissolution−precipitation mechanism) and another involving the reaction between the solid titanium source (often TiO_2) and soluble barium species (the in situ heterogeneous transformation mechanism).[16] The data used previously to study the kinetics of barium titanate crystallization were derived entirely from quenching experiments, whereby material was removed from the reaction vessel after given periods of time and examined. Some workers have used X-ray diffraction analysis to determine the "fractional crystallinity" of solid product formed after various periods of time and hence fractional extent of reaction,[16,17] and others have used electron microscopy to examine the microstructure of materials isolated from the reaction vessel.[18,19]

To shed further light on the mechanism of hydrothermal crystallization of barium titanate powders we have used neutron diffraction to follow the reaction in situ and thus to observe the formation of the crystalline solid in real time and under genuine laboratory conditions. Continual monitoring of the reactions as they take place provides reliable kinetic data in an efficient manner, and avoids the problem that material recovered from a cell in a quenching experiment might have changed irreversibly on cooling and washing and not represent the material present under reaction conditions. To be able to perform in situ studies under the experimentally challenging conditions of a hydrothermal reaction it is necessary to design and construct specialized apparatus, so that data can be measured from laboratory-sized reaction cells in a noninvasive manner.[20,21] Although X-ray diffraction techniques for following hydrothermal crystallizations in situ have been available for several years now,[20−23] this method is not always appropriate for the study of highly absorbing materials. Neutron diffraction offers an alternative means of following crystallizations in a hydrothermal reaction cell, because null-scattering materials are available, whose physical properties are appropriate for the construction of pressure vessels and which give rise to very low background signal. In addition, many materials which have high X-ray absorption cross sections absorb neutrons only weakly. However, time-resolved neutron diffraction has received relatively little attention for the in situ study of chemical reactions under nonambient conditions compared with X-ray diffraction,[24,25] and this is largely due to the fact that data must be collected over long periods of time (minutes rather than seconds possible for X-ray diffraction experiments). We have recently described the construction of the Oxford/ISIS hydrothermal cell from which neutron diffraction data may be recorded during crystallizations[26,27] and reported preliminary results from the first in situ study of barium titanate crystallization.[28] With the ongoing development of rapid neutron diffraction data collection technology we have explored the technique further, and in this paper we present a full account of our time-resolved in situ studies of the hydrothermal crystallization of barium titanate, $BaTiO_3$, performed by using two of the highest count rate neutron diffractometers currently available.

Experimental Section

Materials. Because of the large incoherent scattering arising from protons in a neutron diffraction experiment is it usual to use materials where as many protons as possible are replaced by deuterons so that powder diffraction data with reduced background are measured. All barium titanate crystallizations were therefore performed in D_2O (Fluorchem Ltd). For the first series of experiments, the barium source was perdeuterio barium hydroxide octahydrate, $Ba(OD)_2{\cdot}8D_2O$. This was synthesized by reaction between barium oxide (Aldrich 97+%) and D_2O under a dry nitrogen atmosphere. A mixture of BaO (5 g) and D_2O (30 cm^3) was stirred for ~1 h and the precipitation of $Ba(OD)_2{\cdot}8D_2O$ effected by the addition of dry acetone. The fine white powder was recovered by suction filtration and dried at the pump under a flow of dry nitrogen. The dry nitrogen atmosphere was necessary not only to prevent exchange of deuterated species with atmospheric water vapor but also to prevent the facile reaction between the fine barium deuterioxide powder and atmospheric carbon dioxide, which would give barium carbonate as an impurity. It has also been shown previously that $BaCO_3$ will always form as an impurity if CO_2 is present in the starting materials for hydrothermal synthesis of barium titanate.[29] Batches of accurately weighed $Ba(OD)_2{\cdot}8D_2O$ (~9 g) were prepared and stored in sealed containers under nitrogen before the neutron diffraction experiment. Two titanium sources were used: anatase (TiO_2; Aldrich 99.9%) and amorphous hydrated titania ($TiO_2{\cdot}H_2O$; 99+%, Mitsuwa Chemicals). The latter material has been used recently to prepare submicron particles of *t*-$BaTiO_3$,[4] and was used as supplied as the relatively small amount of protons compared to the large amount of deuterated solvent was found to have little effect on the quality of the diffraction data later obtained. In a second series of experiments, anhydrous barium chloride, $BaCl_2$, was used as supplied by Aldrich (99.9%), and its reaction with anatase carried out in sodium deuterioxide solution (40% in D_2O, supplied by Aldrich, diluted with additional D_2O to give the desired concentration). In all cases the identification of the crystalline solid reagents was confirmed by powder X-ray diffraction measurements.

The Hydrothermal Reaction Cell. A detailed description of the construction and operation of the Oxford/ISIS hydrothermal neutron diffraction cell has been given previously;[26] we will only briefly outline the apparatus here. The cell is similar in volume to commonly used laboratory autoclaves (~25 mL), but is constructed from a Ti−Zr alloy whose "null-scattering" composition (67.7 atm % Ti, 32.3 atm % Zr) results in a material with an average neutron scattering length of zero, yet which is able to contain the pressures generated in a typical hydrothermal reaction at temperatures up to 250 °C. Therefore, the cell gives rise to only a small background signal, it produces no observable Bragg reflections, and the only peaks seen in a diffraction pattern are those arising from crystalline reactant and product phases. The cell is heated top and bottom by copper heating blocks, allowing a large (4 cm high) window to be exposed to the neutron beam (see Figure 1), and is coated internally with a 10 μm layer of gold metal to prevent corrosion of the cell walls by the chemicals used in hydro-

(14) Venigalla, S.; Clancy, D. J.; Miller, D. V.; Kerchner, J. A.; Costantino, S. A. *Am. Ceram. Soc. Bull.* **1999**, *78*, 51.
(15) Hertl, W. *J. Am. Ceram. Soc.* **1988**, *71*, 879.
(16) Eckert, J. O.; Hung-Houston, C. C.; Gerstan, B. L.; Lenka, M. M.; Riman, R. E. *J. Am. Ceram. Soc.* **1996**, *79*, 2929.
(17) Kernchner, J. A.; Moon, J.; Chodelka, R. E.; Morrone, A. A.; Adair, J. H. *ACS Symp. Ser.* **1998**, *681*, 106.
(18) Pinceloup, P.; Courtois, C.; Vicens, J.; Leriche, A.; Thierry, B. *J. Eur. Ceram. Soc.* **1999**, *19*, 973.
(19) MacLaren, I.; Ponton, C. B. *J. Eur. Ceram. Soc.* **2000**, *20*, 1267.
(20) Cheetham, A. K.; Mellot, C. F. *Chem. Mater.* **1997**, *9*, 2269.
(21) Walton, R. I.; D. O'Hare *Chem. Commun.* **2000**, 2283.
(22) Evans, J. S. O.; Francis, R. J.; O'Hare, D.; Price, S. J.; Clarke, S. M.; Flaherty, J.; Gordon, J.; Nield, A.; Tang, C. C. *Rev. Sci. Instrum.* **1995**, *66*, 2442.
(23) Norby, P. *Mater. Sci. Forum* **1996**, *228*, 147−152.
(24) Christensen, A. N.; Convery, P.; Lehamnn, M. S. *Acta Chem. Scand.* **1980**, *A34*, 771.
(25) Polak, E.; Munn, J.; Barnes, P.; Tarling, S. E.; Ritter, C. *J. Appl. Crystallogr.* **1990**, *23*, 258.
(26) Walton, R. I.; Francis, R. J.; Halasyamani, P. S.; O'Hare, D.; Smith, R. I.; Done, R.; Humpreys, R. *Rev. Sci. Instrum.* **1999**, *70*, 3391.
(27) Walton, R. I.; Smith, R. I.; O'Hare, D. *Microporous Mesoporous Mater.* **2001**, *48*, 79.
(28) Walton, R. I.; Smith, R. I.; Millange, F.; Clark, I. J.; Sinclair, D. C.; O'Hare, D. *Chem. Commun.* **2000**, 1267.
(29) Lencka, M.; Riman, R. E. *Chem. Mater.* **1993**, *5*, 61.

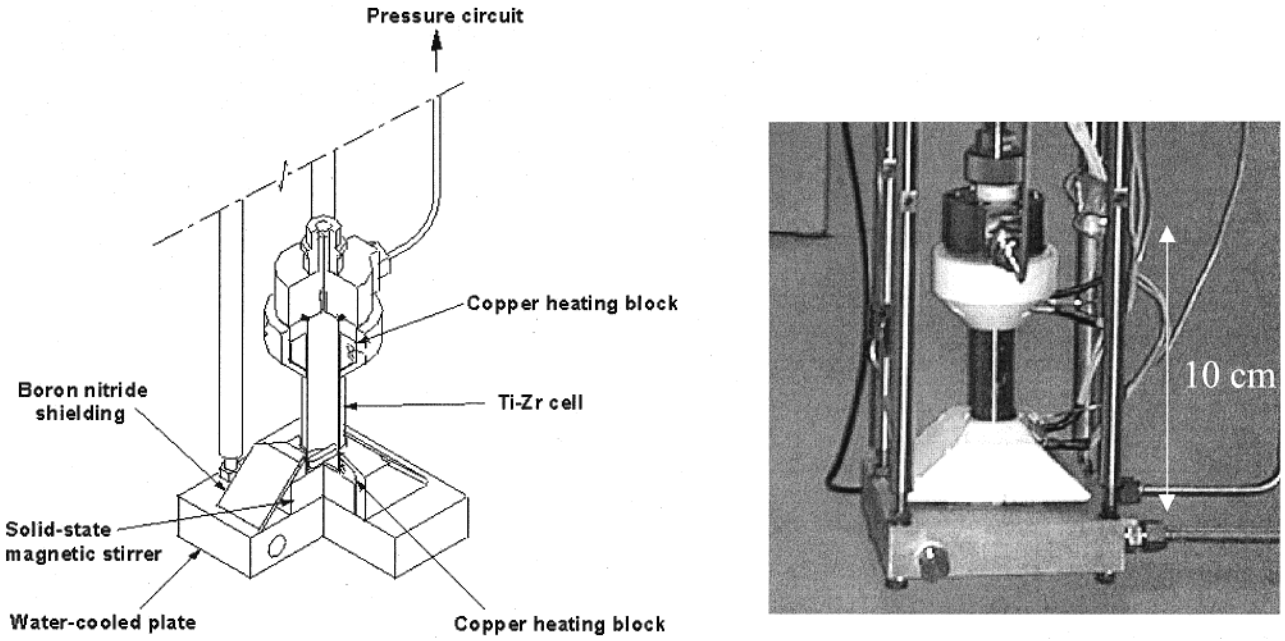

Figure 1. The Oxford/ISIS hydrothermal reaction cell for recording in situ neutron powder diffraction data. Left: A schematic of the reaction vessel. Right: A photograph of the assembled apparatus.

Table 1. Reaction Mixtures Used in the in Situ Neutron Diffraction Studies

experiment	diffractometer	reaction mixture[a]	temp, °C	pressure/bar
ISIS1	POLARIS	2.12 g TiO_2, 9.81 g $Ba(OD)_2{\cdot}8D_2O$, 10 g D_2O	125	2.30
ISIS2	POLARIS	1.66 g TiO_2, 7.59 g $Ba(OD)_2{\cdot}8D_2O$ 10 g D_2O	140	3.13
ISIS3	POLARIS	2.36 g $TiO_2{\cdot}H_2O$, 9.57 g $Ba(OD)_2{\cdot}8D_2O$, 10 g D_2O	125	2.39
ILL1	D20	3.20 g TiO_2, 10 g $BaCl_2$, 6.56 g NaOD, 16 g D_2O	200	7.29
ILL2	D20	3.20 g TiO_2, 10 g $BaCl_2$, 6.56 g NaOD, 16 g D_2O	180	5.24
ILL3	D20	3.20 g TiO_2, 10 g $BaCl_2$, 6.56 g NaOD, 16 g D_2O	150	2.62
ILL4	D20	3.20 g TiO_2, 10 g $BaCl_2$, 6.56 g NaOD, 16 g D_2O	125	1.96
ILL5	D20	3.20 g TiO_2, 10 g $BaCl_2$, 8.75 g NaOD, 13.81 g D_2O	200	5.38
ILL6	D20	3.20 g TiO_2, 10 g $BaCl_2$, 4.37 g NaOD, 18.19 g D_2O	200	9.01

[a] NaOD was used as supplied as a 40% solution in D_2O.

thermal synthesis. The required amounts of reagents were transferred to the hydrothermal cell under a flow of dry nitrogen and the apparatus assembled immediately. Heating to the desired constant temperature from room temperature is typically achieved in around 5 min. The temperature of the heating blocks and the pressure within the cell are monitored continually during reactions.

Time-of-Flight Neutron Diffraction Experiments. Data were collected on the POLARIS diffractometer at ISIS, the UK pulsed spallation neutron source. POLARIS is a medium-resolution, high-intensity powder diffractometer, with a large detector coverage,[30] making it particularly suited for kinetic studies, where data must be acquired in a short period of time in order to collect as many diffraction patterns as possible during a reaction. In the current study, the reaction between barium deuterioxide and either crystalline anatase or amorphous hydrated titania was studied (see Table 1). All reaction mixtures contained a slight excess of barium (Ba:Ti of 1.1:1) as it has been noted previously that an excess of barium is necessary for the complete consumption of the titanium source.[4] Diffraction patterns collected in the POLARIS backscattering detector bank were used in all data analysis. The backscattering detector bank is made up of an array of 58 ^{3}He tubes, covering an angular range of 130−160° in 2θ, thus giving access to a *d*-spacing range of ∼0.2−3.2 Å in the 20 ms time interval between successive neutron pulses from the ISIS target. Neutron diffraction data were processed and manipulated by using the program Genie,[31] which enabled output of data in a format appropriate for the profile fitting program FullProf[32] and also allowed sequential Gaussian-fitting of Bragg reflections to be performed in order to determine their changing area with time during a reaction. It will be useful to note that in the time-of-flight experiment, the *d* spacing of a characteristic Bragg reflection (in Å) is related to time-of-flight (t in μs) by the equation $d = (1.977 \times 10^{-3}/L \sin\theta)t$, where L is the total flight path of the neutron from source to sample to detector element (in m) and 2θ is the Bragg scattering angle. For the backscattering bank on POLARIS, detectors have L ranging from 0.65 to 1.35 m and 2θ from 130 to 160°. Normalization and conversion of time-of-flight to *d* spacing is performed within the program Genie.

Constant-Wavelength Neutron Diffraction Experiments. These studies were performed with use of the D20 diffractometer at the Institut Laue Langevin (Grenoble, France).[33] D20 is a high-flux neutron diffractometer with a 160° position-sensitive detector. This detector has a total of 1600 cells connected to a fast data acquisition system, which allows counting rates of up to 50 000 s^{-1}. The intrinsic time resolution of the detector is at most 40 μs. The combination of high flux and short counting time makes the instrument very well suited for time-resolved studies of changes in sample crystallinity. A primary aim of our experiments was to improve the time resolution of the in situ experiment, i.e. to measure diffraction patterns of sufficient quality for phase identification in shorter periods of time. This would allow more accurate crystallization curves to be obtained, with a greater number of data points for a given reaction, and also more rapid reactions could

(30) Hull, S.; Smith, R. I.; David, W. I. F.; Hannon, A. C.; Mayer, J.; Cywinski, R. *Physica B* **1992**, *180* and *181*, 1000.

(31) David, W. I. F.; Johnson, M. W.; Knowles, K. J.; Smith, C. M. M.; Crosbie, G. D.; Campbell, E. P.; Graham, S. P.; Lyall, J. S. Rutherford Appleton Laboratory Report RAL-86-102, 1986.

(32) Rodriguez-Carvajal, J. In *Satellite Meeting on Powder Diffraction*, Abstracts of the XVth Conference of the International Union of Crystallography, Toulouse, 1990, p 127.

(33) Convert, P.; Hansen, T.; Oed, A.; Torregrossa, J. *Physica B* **1998**, *241−243*, 195.

be studied, for example, those taking place at higher temperature. Data were thus collected from reactions performed at 100−200 °C in time intervals of 5 min. In addition, for this second series of experiments we chose to use a different source of barium, $BaCl_2$. This material could be used as supplied, and because sodium deuterioxide is also required in this case, we could easily investigate the effect of deuterioxide ion concentration on the course and kinetics of the hydrothermal reaction. Table 1 contains details of the starting materials and reaction conditions employed in these experiments. An incident neutron wavelength of 1.3 Å was selected by using a Cu(200) monochromator. At this wavelength the monochromatic beam has its highest flux ($\sim 6 \times 10^7$ neutrons $cm^2\ s^{-1}$).

Results

Time-of-Flight Diffraction Studies. Figure 2 shows neutron powder diffraction patterns of the crystalline starting materials. Data were collected from dry powders of TiO_2 (Figure 2a) and $Ba(OD)_2 \cdot 8D_2O$ (Figure 2b) held in 11 mm vanadium cans and from a typical reaction mixture in the Ti−Zr hydrothermal cell before heating (Figure 2c). The data were analyzed by using a whole pattern-fitting algorithm in order to determine accurately the profile shape function, background, and cell parameters. It was confirmed by the good fit achieved to the diffraction data that the TiO_2 is present purely in the anatase polymorph. The structure of barium hydroxide octahydrate has been determined by Sacerdoti et al. using single-crystal X-ray diffraction methods,[34] and using their cell parameters as a starting point for refinement against our neutron diffraction data allowed confirmation of the identity of the barium source (X-ray values: $a = 9.274$ Å, $b = 9.260$ Å, $c = 11.817$ Å, $\beta = 98.95°$;[34] neutron refined values: $a = 9.3137$ (3) Å, $b = 9.3043(3)$ Å, $c = 11.860(8)$ Å, $\beta = 98.995(3)°$). The diffraction data of the starting mixture (2.12 g of TiO_2, 9.81 g of $Ba(OD)_2 \cdot 8D_2O$, and 10 g of D_2O) could be fitted satisfactorily as arising from a mixture of TiO_2 and $Ba(OD)_2 \cdot 8D_2O$, as expected. This demonstrates that, although addition of the solvent causes an increase in the background in the diffraction data, unambiguous identification and refinement of cell parameters is possible from crystalline solids mixed with D_2O in the Oxford/ISIS hydrothermal cell, and that the cell exhibits no contaminating Bragg reflections.

Figure 3 shows a stack plot of powder neutron diffraction data recorded during the crystallization of barium titanate at 125 °C during experiment ISIS1 (see Table 1). The hydrothermal bomb was filled to ~50% of its total volume. This temperature was chosen as it is below the Curie point, where the ferroelectric tetragonal form is thermodynamically most stable. The first pattern was recorded at room temperature before heating, the second during heating to 125 °C, and the later patterns under isothermal conditions every 15 min. Before considering the course of this reaction, we will discuss first the nature of the final product. Figure 4 shows the sum of the four final diffraction patterns obtained, i.e. 1 h of accumulated data in total. These data can be successfully modeled as arising from cubic $BaTiO_3$, even though the temperature studied is below the Curie temperature, where we would expect *t*-$BaTiO_3$ to have formed. In the powder diffraction pattern this cubic to tetragonal phase transformation is characterized by a splitting of certain Bragg reflections in the tetragonal form, and this is a common means of distinguishing these two polymorphs of $BaTiO_3$.[35] The tetragonal splitting is small, however, and the Bragg reflections are broadened considerably due to the small (submicron) particles of $BaTiO_3$. Difficulties might therefore be expected in using data collected on a medium resolution diffractometer such as POLARIS to identify the $BaTiO_3$ polymorph. Certain authors have suggested that the intrinsic strain of the tetragonal polymorph cannot be supported by very small particles[36] and that the entrapment of hydroxyl groups in the lattice favors the

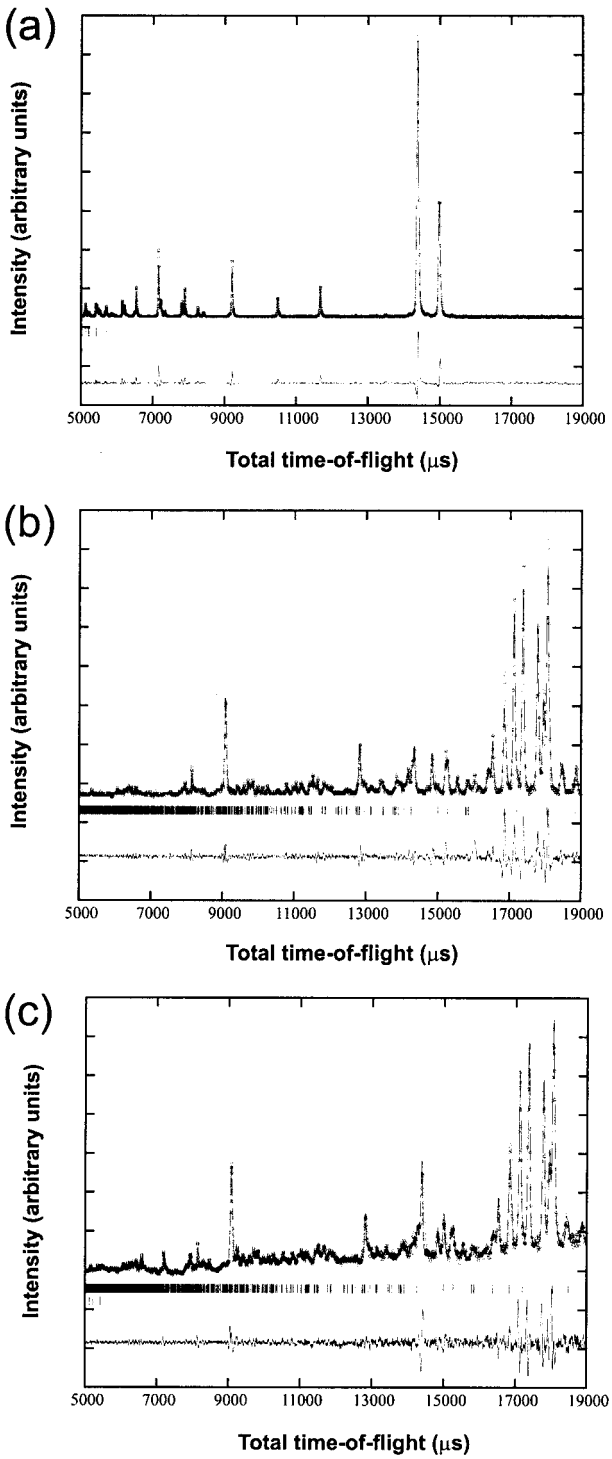

Figure 2. Neutron powder diffraction patterns of starting materials: (a) TiO_2 powder in a vanadium can, 30 min data collection; (b) $Ba(OD)_2 \cdot 8D_2O$ powder in a vanadium can, 30 min data collection; and (c) TiO_2 and $Ba(OD)_2 \cdot 8D_2O$ with D_2O in the hydrothermal cell. Fits obtained by refinement of cell parameters are shown; in each case, the points are the experimental data, the full line the result of the whole pattern fitting, and the lower curve the difference plot.

(34) Sacerdoti, M.; Bertolasi, V.; Ferretti, V.; Accorsi, C. A. *Z. Kristallogr.* **1990**, *192*, 111.

(35) Shi, E. W.; Xia, C. T.; Zhong, W. Z.; Wang, B. G.; Feng, C. D. *J. Am. Ceram. Soc.* **1997**, *80*, 1567.

(36) Uchino, K.; Sadanaga, E.; Hirose, T. *J. Am. Ceram. Soc.* **1989**, *72*, 1555.

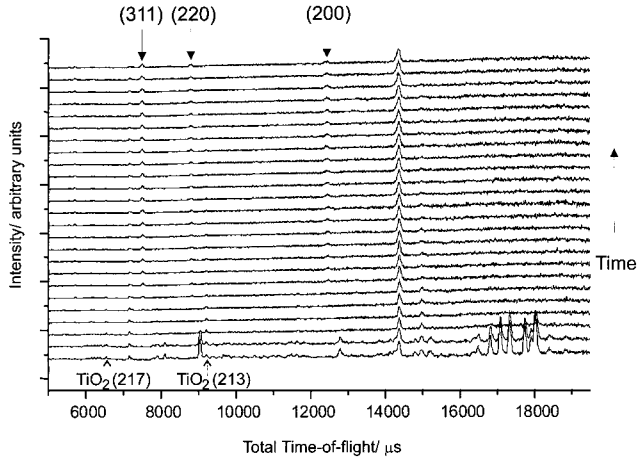

Figure 3. Neutron powder diffraction patterns measured in 15 min intervals from within the hydrothermal cell during the reaction between $Ba(OD)_2 \cdot 8D_2O$ and TiO_2 in D_2O at 125 °C. The arrows show the positions of well-resolved Bragg reflections due to the $BaTiO_3$ product later integrated for kinetic analysis, and of the TiO_2 starting material.

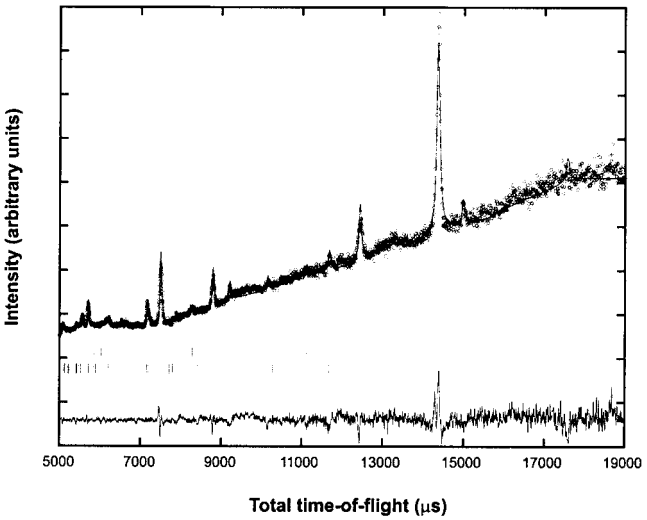

Figure 4. Time-of-flight neutron powder diffraction data measured during the final hour of the barium titanate crystallization at 125 °C. The fit obtained by refinement of cell parameters of cubic barium titanate and unreacted TiO_2 is shown (key as for Figure 2).

formation of the cubic form;[37] however, studies involving methods other than diffraction, such as recent work with Raman spectroscopy,[4] show convincingly that submicron particles of *t*-$BaTiO_3$ can be formed by the hydrothermal route. It must be assumed, therefore, that a combination of diffractometer resolution and a broadening of the Bragg reflections due to the small particle size prevents us from resolving the tetragonal splitting of the reflections in our diffraction study. This explains why the neutron diffraction data measured in situ from the barium titanate at 125 °C can be satisfactorily modeled as arising from the cubic polymorph. It should be noted that the refined cell parameter of 4.03(2) Å has been determined at 125 °C and is slightly larger than determined at room temperature (3.99 Å), as expected with thermal expansion. We can also use the data from the final product to examine the difference between the $BaTiO_3$ prepared when $TiO_2 \cdot H_2O$ is used as the titanium source at 125 °C, instead of anatase, TiO_2. Previous work has shown recently that using this amorphous titanium source allows the preparation of smaller particles of $BaTiO_3$ than when crystalline

(37) Vikekanandan, R.; Kuuty, T. R. N. *Powder Technol.* **1989**, *57*, 181.

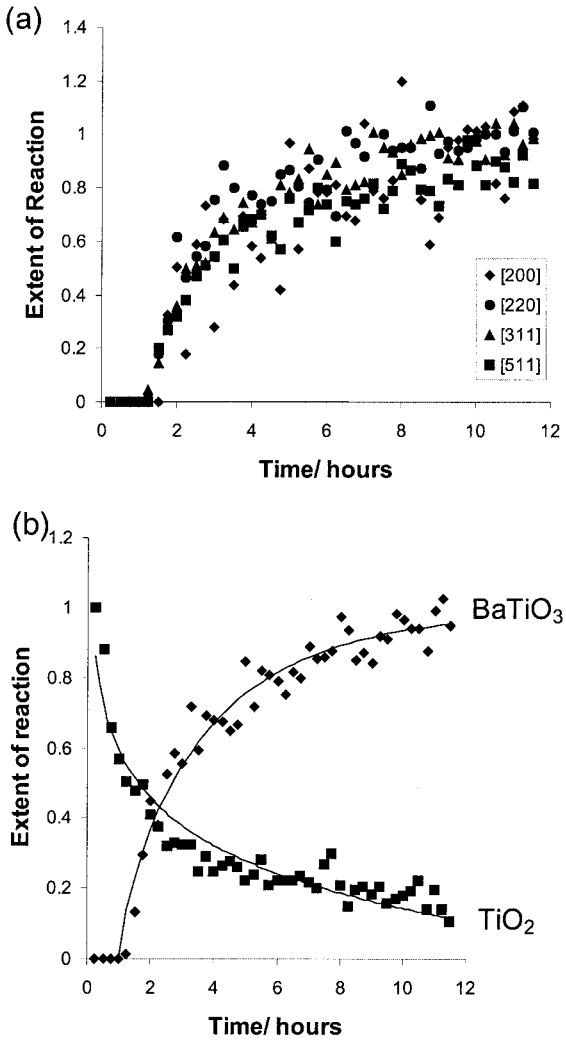

Figure 5. (a) Normalized growth curves for four barium titanate Bragg reflections for the reaction at 125 °C. (b) Average growth curve for barium titanate and the decay curve of TiO_2. Lines are for guidance only and have no mathematical significance.

anatase is used,[4] and the larger peak width (fwhm) fitted to the refined data is consistent with this (106 μs for the anatase-derived product and 140 μs for the amorphous titania product).

The integrated intensities of well-resolved Bragg reflections were determined by Gaussian fitting to enable decay and growth curves of starting materials and products to be produced. The most intense Bragg reflection of $BaTiO_3$ (the (111) at ~14300 μs) coincides with strong reflections of both TiO_2 and $Ba(OD)_2 \cdot 8D_2O$, but it was possible to select four reflections of $BaTiO_3$ (the (200) at ~12400 μs, the (220) at ~8675 μs, the (311) at ~7500 μs, and the (511) at ~4800 μs) and two of TiO_2 (the (217) at ~6550 μs and the (213) at ~9220 μs) which showed no overlap with nearby reflections. Figure 5a shows the normalized growth curves produced by this analysis. Normalization was achieved by dividing the data by the average peak intensity of the last eight points, assuming that growth of barium titanate had ceased by this point. It is apparent from Figure 5a that the normalized growth curves from four different Bragg reflections of $BaTiO_3$ are coincident. This suggests that crystal growth is isotropic, which is not unexpected given the spherical morphology of particles typically produced by the hydrothermal route.[4,19] The four curves were thus averaged to produce the growth curve shown in Figure 5b, which also shows the decay curve for TiO_2, normalized to the intensity of the studied Bragg

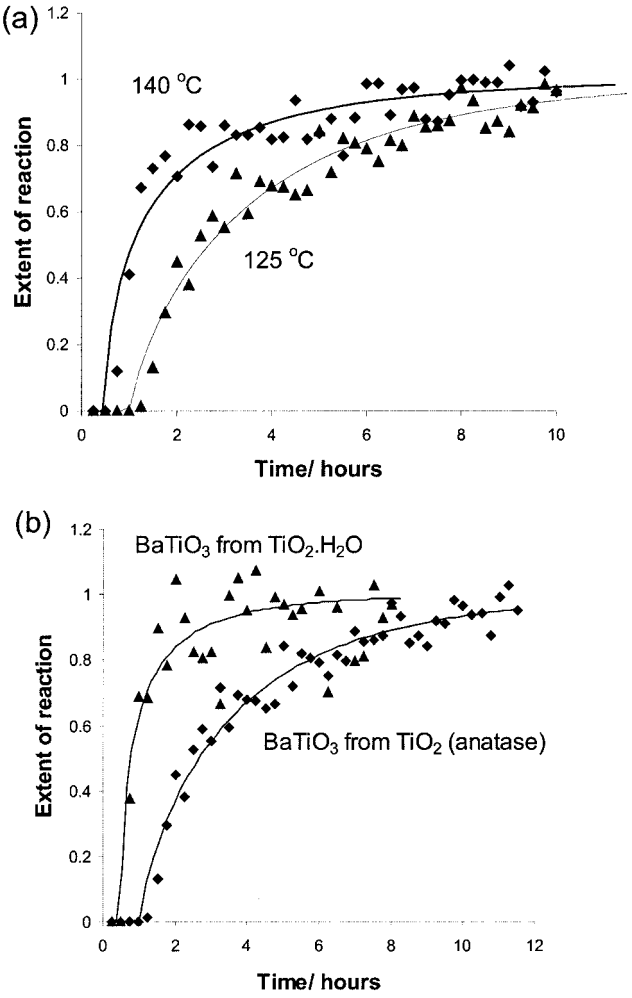

Figure 6. Growth curves of barium titanate from crystalline TiO_2 at (a) two temperatures and (b) using two different titanium sources at 125 °C. Lines are only guides to the eye and have no physical significance.

reflection before heating. It is apparent that the reaction has not gone to completion because Bragg reflections from TiO_2 are still present at the end of the heating period.

The reaction was repeated at higher temperatures, and the barium titanate growth curve produced at 140 °C is shown, along with that at 125 °C for comparison, in Figure 6a. At temperatures higher than 140 °C, the reactions were much more rapid, as expected, and it was difficult to measure sufficient points to describe a growth curve, given the time resolution of the experiment (for example, at 180 °C the reaction appears complete after only 1 h, and four diffraction patterns). Figure 6b shows the growth curve obtained when the amorphous titanium source $TiO_2 \cdot H_2O$ is used. The enhancement of reaction rate is immediately obvious from these data. When using the amorphous titanium source there is no means of tracking its decay with the diffraction technique, since it exhibits no distinct diffraction features. However, integration over the region expected for Bragg reflections of TiO_2 was performed in order to test whether diffracted intensity from the $Ba(OD)_2 \cdot 8D_2O$ Bragg reflections contributed to the data. It was thus shown that only intensity from anatase reflections could account for the fitted intensity in the regions fitted, and so the decay curves for the crystalline TiO_2 previously deduced were correct. This was important to establish as we wished to determine the behavior of TiO_2 during the early stages of reaction. The growth

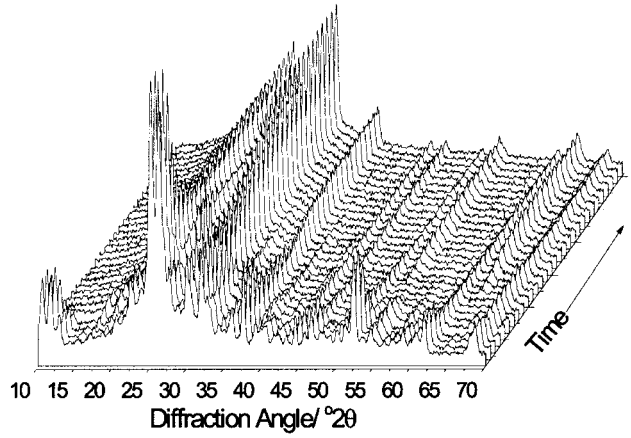

Figure 7. 3D plot of constant-wavelength neutron data measured during the reaction between TiO_2 and $BaCl_2$ in $NaOD/D_2O$ at 180 °C (Experiment ILL1, Table 1).

curves deduced in these experiments contain valuable qualitative information about the course of crystallization, but the relatively few data points make extraction of quantitative kinetic data very difficult. Thus we have used our second set of experiments, on the D20 diffractometer at the ILL, France, to investigate this line of data analysis.

Constant-Wavelength Diffraction Studies. Figure 7 shows a three-dimensional representation of neutron powder diffraction data measured during the formation of barium titanate from $BaCl_2$ and TiO_2 in $NaOD/D_2O$ solution at 180 °C on the D20 diffractometer. The shorter time interval (5 min) and the improved signal-to-noise ratio of the data in this series of experiments allows the diffraction patterns to be plotted in this form, and changes between patterns are immediately apparent. Almost immediately after commencement of heating, the characteristic Bragg reflections of the crystalline source of $BaCl_2$ begin to decay, and within four diffraction patterns (20 min) have disappeared completely. It is unfortunate that the complexity of the diffraction data from $BaCl_2$ obscures features due to TiO_2 at the early stages of reaction. However, it can be seen that although TiO_2 Bragg reflections start to diminish in intensity at the beginning of the experiment, they do so much more slowly than the features due to $BaCl_2$: for example, the Bragg reflection at $2\theta \sim 48°$ (see Figure 8). These observations are consistent with the results from the previous set of experiments, but it proved impossible to extract meaningful decay curves for TiO_2 from the fixed wavelength data because of overlap of all Bragg reflections with nearby features due to $BaCl_2$. Instead, we concentrate on determining accurate crystallization curves describing the formation of $BaTiO_3$.

The most intense Bragg reflections of $BaTiO_3$ overlap with features of either $BaCl_2$ or TiO_2 (or both phases); for example, the 111 reflection ($2\theta \approx 32°$) overlaps with three strong Bragg reflections of TiO_2 (the 103, 004, and 112) so it appears that the diffracted intensity in this region has constant intensity throughout the experiment. The 311 reflection of $BaTiO_3$, centered at $2\theta \approx 64.0°$ provided the most accurate growth curves. It should be noted that at temperatures above 130 °C, $BaTiO_3$ exists as the metastable cubic polymorph and so splitting of this peak into separate 311 and 113 reflections should not be observed, and we can determine its area using a single Gaussian function. Figure 8a shows crystallization curves determined at three temperatures when the reaction clearly reaches completion within the detection limits of the experiment. The data were normalized to the average intensity of the last

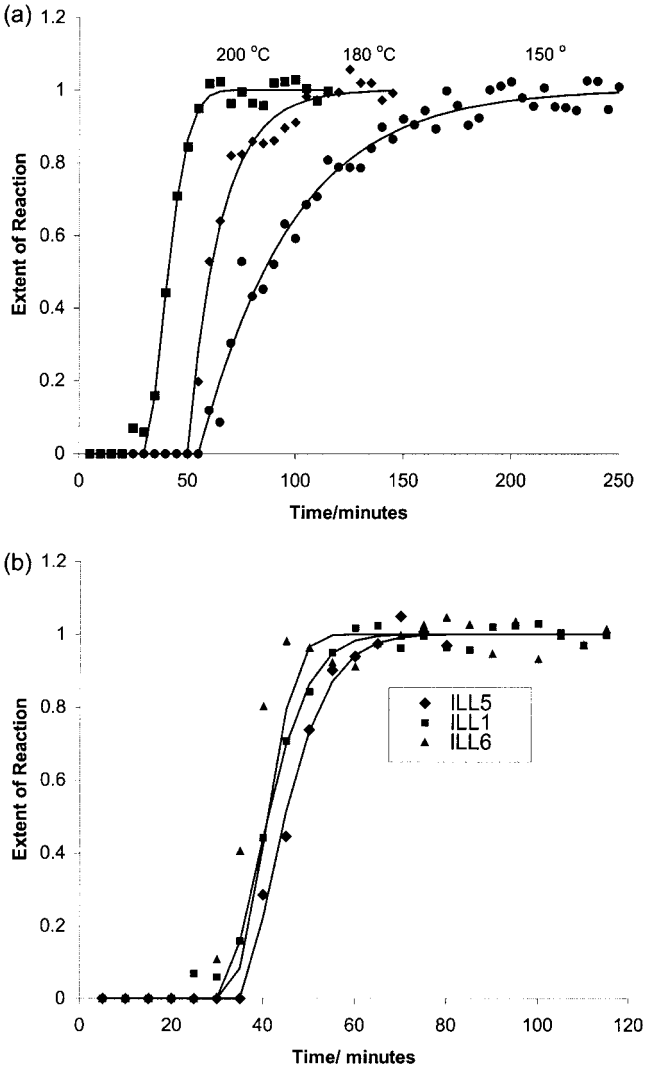

Figure 8. Crystallization curves for $BaTiO_3$ (a) determined at three different temperatures for the reaction between TiO_2 and $BaCl_2$ in $NaOD/D_2O$ and (b) determined at 200 °C at three NaOD concentrations. Lines are those derived by fitting to the Avrami−Erofe'ev crystallization model.

four data points, and the amount of barium titanate has reached a maximum, constant value in each case. For the experiments performed at 125 °C the crystallization is considerably slower and we have only noted the time taken for the first barium titanate Bragg reflections to appear (see below). For the reactions performed with different concentrations of NaOD the data were analyzed in the same manner and the growth curves for barium titanate are shown in Figure 8b. It should be noted that in these studies although the total volume of the reaction mixture was similar, and the temperature maintained at 200 °C, the final pressure achieved varied (which is presumably due to the differing salt concentrations in the cell). It is apparent that halving or doubling the amount of NaOD in the reaction mixture has little effect on the induction time for crystallization or on the time taken for the reaction to reach completion.

To extract quantitative kinetic information about the barium titanate crystallizations the growth curve data were treated using the Sharp−Hancock method.[38] This method has successfully been applied to model kinetic data from a variety of hydrothermal crystallizations, and most importantly allows a rate constant to be determined to enable the effect of reaction

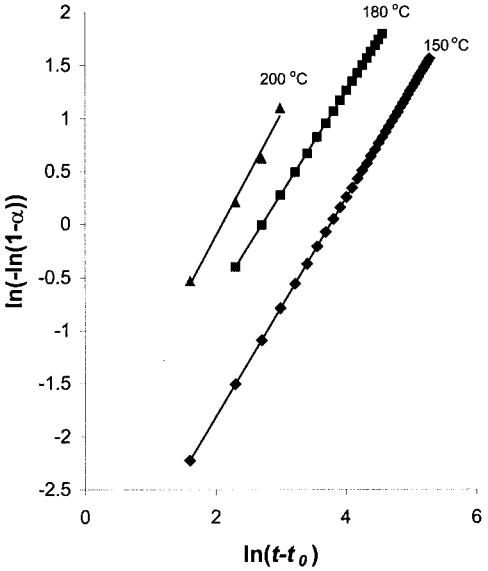

Figure 9. Sharp−Hancock plots for the crystallization of barium titanate at three temperatures. The lines were derived by linear regression.

conditions on the kinetics of a reactions to be seen easily.[39−41] Starting from the Avrami−Erofe'ev expression for a nucleation-growth crystallization mechanism, eq 1,[42−45] Sharp and Hancock derived an expression from which it is possible to extract kinetic information from the gradient and intercept of a linear graph, eq 2.

$$\alpha = 1 - \exp\{-(k(t - t_0))^n\} \quad (1)$$

$$\ln[-\ln(1 - \alpha)] = n \ln(t - t_0) + n \ln(k) \quad (2)$$

α is the extent of reaction scaled from zero at the beginning of reaction to unity at the end, t the time coordinate, t_0 the induction time for the process studied, k the rate constant, and n the Avrami exponent. Thus a graph of $\ln[-\ln(1 - \alpha)]$ vs $\ln(t - t_0)$ will have a gradient n and y-axis intercept of $n \ln(k)$ over the region where the nucleation-growth model applies. The model was originally developed to describe the growth of crystallites in solid−solid reactions, and assumes the formation of nucleation sites in a uniform mixture of reagents from which crystal growth occurs. Most importantly, Sharp and Hancock showed that linear graphs will be produced for $0.15 < \alpha < 0.5$ for a large number of other limiting cases of crystal growth, and that the value of n allows one to distinguish whether a reaction is diffusion controlled or phase boundary controlled, or whether the formation of nucleation sites is the rate determining step for crystal growth.[38] In our analysis, t_0 was fixed at the time observed for the first appearance of Bragg reflections of barium titanate, and linear regression was used to determine the gradient and intercept of Sharp-Hancock plots. These are shown in Figure 9, and the kinetic parameters extracted with this method of data analysis are contained in Table 2.

Although we have modeled kinetic data at only three different temperatures, we used the rate constants to determine an activation energy for barium titanate crystallization. The Ar-

(38) Hancock, J. D.; Sharp, J. H. *J. Am. Ceram. Soc.* **1972**, *55*, 74−77.
(39) Thompson, R. W. *Zeolites* **1992**, *12*, 681.
(40) Francis, R. J.; O'Brien, S.; Fogg, A. M.; Halasyamani, P. S.; O'Hare, D.; Loiseau, T.; Ferey, G. *J. Am. Chem. Soc.* **1999**, *121*, 1002.
(41) Norby, P.; Hanson, J. C. *Catal. Today* **1998**, *39*, 301−309.
(42) Avrami, M. *J. Chem. Phys.* **1939**, *7*, 1103.
(43) Avrami, M. *J. Chem. Phys.* **1940**, *8*, 212.
(44) Avrami, M. *J. Chem. Phys.* **1941**, *9*, 177.
(45) Erofe'ev, B. V. *C. R. Dokl. Acad. Sci. URSS* **1946**, *52*, 511.

Table 2. Kinetic Parameters Determined by Analysis of the Crystallization Curves Using the Sharp and Hancock Method[a]

reaction[b]	t_0, min	k, min^{-1}	n
ILL1	35	0.122	1.15
ILL2	50	0.066	0.98
ILL3	55	0.023	1.03
ILL4[c]	135		

[a] t_0 is the induction time for crystallization, k the rate constant for crystallization, and n is the Avrami exponent. [b] See Table 1. [c] This reaction did not go to completion so only t_0 is noted.

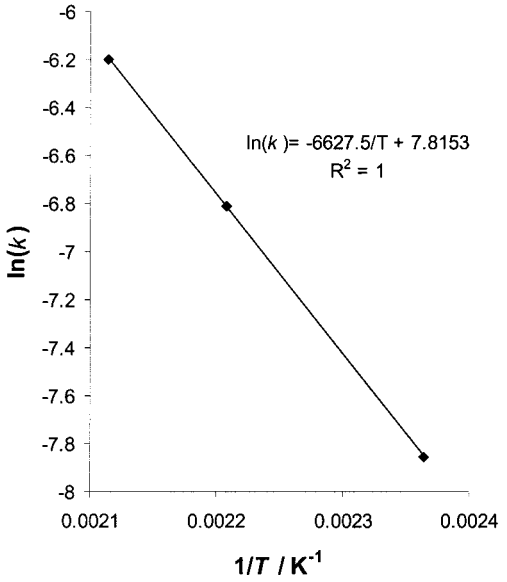

Figure 10. An Arrhenius plot for hydrothermal barium titanate crystallization.

rhenius plot obtained is shown in Figure 10; the linearity of the plot gives us further confidence in the kinetic analysis we have performed. The activation energy determined by linear regression is 55.10 kJ mol^{-1}.

Hertl used an alternative mathematical model for the kinetics of barium titanate crystallization.[15] Instead of assuming the formation of nucleation sites in a uniform mixture of reactive species, he used an "area dependence model" by considering the reaction between solution $Ba^{2+}_{(aq)}$ cations and solid TiO_2 particles. By taking into account the increasing thickness of the product layer and the decreasing surface area of the reactant, and assuming particles are spherical, application of Fick's first law of diffusion leads to the expression:

$$1 - {}^2/_3\alpha - (1-\alpha)^{2/3} = kt/r_0{}^2 \qquad (3)$$

α is the extent of reaction as before, and r_0 is the radius of the particles of the solid reagent at the beginning of the reaction. This equation was first derived by Gistling and Brounshtein to describe diffusion-controlled kinetics in spherical particles.[46] The simple model assumes the presence of monodispersed TiO_2 particles at the beginning of reaction, and clearly knowledge of the particle-size (and particle shape) distribution is necessary to develop a more refined model. Nevertheless, if we assume r_0 represents an average initial particle radius of TiO_2 spheres, a plot of $(1 - {}^2/_3\alpha - (1-\alpha)^{2/3})$ vs $t - t_0$ should yield a straight line of gradient k/r_0 if this heterogeneous area dependence model holds. In each case markedly nonlinear plots were obtained.

(46) Gistling, A. M.; Brounshtein, B. I. *J. Appl. Chem. USSR (Engl. Trans.)* **1950**, *23*, 1327.

Discussion

The first observation from our in situ study is that the crystalline barium source (either $Ba(OD)_2{\cdot}8D_2O$ or $BaCl_2$) dissolves rapidly before any other changes in crystallinity are apparent in the reaction mixture. In all cases the Bragg reflections of $Ba(OD)_2{\cdot}8D_2O$ or $BaCl_2$ are seen to diminish in intensity as soon as heating is started: all of these disappear in less than 1 h and always before the appearance of any crystalline $BaTiO_3$. The solubility of the barium salts in water increases dramatically with increased temperature so it is not unexpected that the materials dissolve under hydrothermal conditions. All previously discussed mechanisms for the hydrothermal crystallization of barium titanate suggest that the barium source is in solution and our in situ results provide clear evidence for this assumption. What is particularly noteworthy about our results is that when crystalline TiO_2 is used as the titanium source its initial decay is rapid and more than 50% of the TiO_2 dissolves before the appearance of any of the $BaTiO_3$ product. This strongly suggests that a dissolution−precipitation mechanism is taking place, at least at the early stages of reaction, i.e. that barium titanate is formed by reaction between solution Ba^{2+} and $Ti(OH)_x{}^{4-x}$ species. It should be noted that there are no data currently available to ascertain particle size during the earliest stage of barium titanate formation, so that the model might more accurately be described as dissolution−crystallization; we use the term dissolution−precipitation to be consistent with previous workers. If the reaction between Ba^{2+} ions in solutions and solid TiO_2 particles was taking place, then we would expect the rate of formation of $BaTiO_3$ to mirror closely the decay of TiO_2. Some authors have previously assumed the latter in situ heterogeneous transformation mechanism,[15] but more recent studies with electron microscopy techniques find no evidence for this model; for example, Pinceloup et al. examined the products of barium titanate crystallizations after various periods of time and always observed distinct titania or barium titanate particles, with no relationship in particle size distribution in the titanium oxide starting material and the barium titanate product.[18] Our study thus provides complementary evidence for the dissolution−precipitation mechanism.

The use of the constant wavelength D20 diffractometer allowed more rapid data collection and we were able to follow crystallizations at higher temperatures, and to measure a larger number of data points describing the lower temperature reactions. Kinetic analysis with the Sharp−Hancock method allows a satisfactory simulation of the barium titanate growth curves. This model is based on a nucleation growth situation, whereby nucleation sites for crystallization form in a uniform mixture of reactive species derived from the starting materials. The value of n is often used to distinguish between different mechanisms of reaction: for $n \sim 0.5$, a diffusion-limited rate is inferred, where the rate of diffusion of reactive species to the nucleation sites is the rate-determining step; for $n \sim 1$ the reaction at the phase boundary between the product and reagent mixture is rate determining and for $n > 1$ the formation of nucleation sites is the process that controls the rate.[38] For the barium titanate crystallization we find that the value of n is ~1, and this shows good agreement for the three different temperatures studied. This suggests that the rate-determining step of reaction is the reaction at the phase boundary, i.e. the chemical reaction taking place at the nucleation sites (small crystallites of $BaTiO_3$) between Ba^{2+} cations and $Ti(OH)_x{}^{4-x}$ anions. Kerchner et al. used the same method of data analysis on crystallization curve data derived by determining fractional crystallinity of quenched samples and found the same value for n.[17] Eckert et al. also

applied the Sharp−Hancock method and suggested two regions of crystal growth are apparent,[16] but with the small amount of data they supplied we believe it is not possible to draw such a conclusion. There is no evidence from our studies for two distinct regions of crystal growth. Previous calculations of activation energies for barium titanate crystallization under hydrothermal conditions include a value of 21 kJ mol^{-1} by Ovramenko et al.[47] and a value of 105.5 kJ mol^{-1} by Hertl et al.[15] Our value of 55 kJ mol^{-1} is comparable, but it should be noted that different titania sources were used is each case. Finally, we note that the poor fit of the simple heterogeneous model for the crystallization kinetics, namely that based on the Gistling and Brounshtein model, is consistent with our conclusion that the homogeneous dissolution−precipitation mechanism dominates in the hydrothermal crystallization of barium titanate.

Conclusions

The use of in situ neutron diffraction allows chemical reactions involving crystalline solids that take place in bulky reaction vessels to be monitored in real time with negligible contamination of the diffraction pattern of the reactants and products with signals from the sample cell. We stress that our hydrothermal reaction cell has similar dimensions to cells available commercially for general laboratory use so that we are able to use quantities of chemicals (grams) used in typical laboratory syntheses, thereby avoiding any problems of reproducibility that potentially could arise from scaling down of reactions to very small volumes. In the case of barium titanate crystallization we can observe directly the consumption of starting materials and the isotropic growth of solid product from solution. These qualitative observations allow us to postulate that a dissolution−precipitation mechanism predominates at the early stages of reaction. The use of the D20 diffractometer with its high incident neutron flux and large position-sensitive detector allows more rapid data collection and we have extracted crystallization curves describing hydrothermal barium titanate formation containing far more data points than any previous studies. This allowed us to extract quantitative kinetic information, such as rate constants, and to test the validity of relevant kinetic models. We envisage that with further developments in neutron diffraction technology in the future, even more rapid data collection will make in situ studies of crystallizations under nonambient conditions a very important technique in elucidating the formation mechanisms of industrially important inorganic materials.

Acknowledgment. We thank the EPSRC for financial support and provision of beam-time at the ISIS Facility, the ILL for provision of beamtime on D20, the D20 technicians for adapting the cell for use at ILL, and Dr. D. C. Sinclair and Mr. I. Clark, Department of Engineering Materials, University of Sheffield, for useful discussions and supplying the amorphous titania material.

JA011805P

(47) Ovramenko, N. A.; Shevts, L. I.; Ovcharenko, F. D.; Kornilovich, B. Y. *Izv. Akad. Nauk SSSR, Neorg. Mater.* **1979**, *248*, 889.